

Magnetic Properties and Structure of Amorphous $\text{Fe}_{74}\text{Hf}_4\text{Ta}_1\text{Cu}_1\text{Gd}_1\text{La}_x\text{Si}_{15-x}\text{B}_4$ ($x = 0, 7$) Ribbons

P.J. BARDZIŃSKI^{a,*}, M. KOPCEWICZ^b, M. RYBACZUK^a, M. HASIAK^a, A. MUSIAŁ^c,
V. KINZHYBALO^d AND B. IDZIKOWSKI^c

^aWrocław University of Technology, Wrocław, Poland

^bInstitute of Electronic Materials Technology, Warsaw, Poland

^cInstitute of Molecular Physics, PAS, Poznań, Poland

^dInstitute of Low Temperature and Structure Research, PAS, Wrocław, Poland

(Received November 16, 2014; in final form December 26, 2014)

The multi component $\text{Fe}_{74}\text{Hf}_4\text{Ta}_1\text{Cu}_1\text{Gd}_1\text{La}_x\text{Si}_{15-x}\text{B}_4$ ($x = 0, 7$) alloys are promising candidates in the search for materials with unusual mechanical and magnetic properties. Amorphous nature of melt-spun samples was confirmed by X-ray diffractometry and Mössbauer spectroscopy. The X-ray diffraction patterns revealed a distinct amorphous halo. The low-field components of magnetic hyperfine field distributions on iron nuclei are observed in the Mössbauer spectra, with average hyperfine field values of 19.9 and 15.7 T for $x = 0$ and $x = 7$, respectively. Coercivity studied by vibrating sample magnetometer was about 12 A/m for $x = 0$ and 82 A/m for $x = 7$ at 300 K and about 600 A/m for $x = 0$ and 1200 A/m for $x = 7$ at 400 K. Remanence also changed with temperature, amounting to 0.64 T for $x = 0$ and 0.36 T for $x = 7$ at 300 K, while at 400 K it was 0.43 and 0.11 T for $x = 0$ and $x = 7$, respectively. It is shown that La addition has beneficial effect of shifting the Curie point towards lower temperatures together with the increase of magnitude of magnetization.

DOI: [10.12693/APhysPolA.127.827](https://doi.org/10.12693/APhysPolA.127.827)

PACS: 75.50.-y, 75.50.Bb, 75.50.Kj, 75.60.Ej, 81.05.Kf, 82.80.Ej, 61.05.Qr

1. Introduction

Multicomponent metallic glasses recently attracted a lot of attention due to their exceptional soft magnetic properties [1], high hardness and elastic modulus, together with improved glass-forming ability [2, 3]. In the present study it was decided to investigate new amorphous alloys with the composition similar to $\text{Fe}_{88}\text{Zr}_7\text{B}_4\text{Cu}_1$ studied by Caballero-Flores et al. [4], known for noticeable peak magnetic entropy change of $1.32 \text{ J kg}^{-1} \text{ K}^{-1}$ at 287 K. The mass percentage of Hf and Zr are equal in the chosen alloy and in the aforementioned work. The composition selected is close to the near-eutectic point in the Fe–Hf phase diagram [5] as well as to the peritectic composition of the Fe–La–Si phase diagram [6, 7], which promotes higher expected glass-forming ability [8]. With such composition, annealing may lead to the formation of $\text{La}(\text{Fe},\text{Si})_{13}$ phase exhibiting giant magnetocaloric effect, that exhibits ferromagnetic to paramagnetic transition at 174 K [9]. The addition of 1 at.% Ta may lead to the formation of $\text{Fe}_2\text{Hf}_{0.835}\text{Ta}_{0.165}$ phase after annealing, with a ferromagnetic to antiferromagnetic transition at around 240 K [10]. Finally, addition of 1 at.% Gd, the element introducing large magnetic moment, could alter the expected ferromagnetic behavior of the alloys studied. The aim of this study is to describe the major structural and magnetic characteristics of the studied systems.

2. Experimental details

Initial Hf–Ta and Fe–Cu–B–Si–Gd–La alloy ingots were prepared by arc-melting of pure elements under Zr-gettered Ar 6.0 atmosphere. Then, the ingots were remelted together four times to homogenize the samples. 1.00 mm wide ribbons of $\text{Fe}_{74}\text{Hf}_4\text{Ta}_1\text{Cu}_1\text{Gd}_1\text{La}_x\text{Si}_{15-x}\text{B}_4$ ($x = 0, 7$) alloys were obtained by single-roller melt spinning method with a copper wheel velocity of 40 m/s and a quartz crucible. The samples were 28 and $34.57 \mu\text{m}$ thick for $x = 0$ and $x = 7$, respectively.

Structure of the samples was initially examined by powder X-ray diffractometry (XRD) on the PANalytical X'Pert diffractometer utilizing $\text{Cu } K_\alpha$ radiation. Then, room temperature Mössbauer measurements were performed in transmission mode using a constant acceleration spectrometer with ^{57}Co -in-Rh source. The isomer shifts were given with respect to bcc iron at room temperature. Hyperfine field distributions were obtained by fitting the Mössbauer spectra with NORMOS.dist program. Thermal stability of the alloys was investigated by differential scanning calorimetry (DSC) at a heating rate of 10 K/min. Magnetic properties of the as-quenched alloys were studied by the vibrating sample magnetometer in a temperature of 50–400 K. The temperature dependence of magnetization was recorded at the fields of 5 mT and 200 mT.

3. Structure and thermal stability

Figure 1 presents powder X-ray diffraction patterns for the as-quenched alloys. The distinctive amorphous halo could be identified between 40° and 50° values of 2θ

*corresponding author; e-mail: piotr.bardzinski@pwr.edu.pl

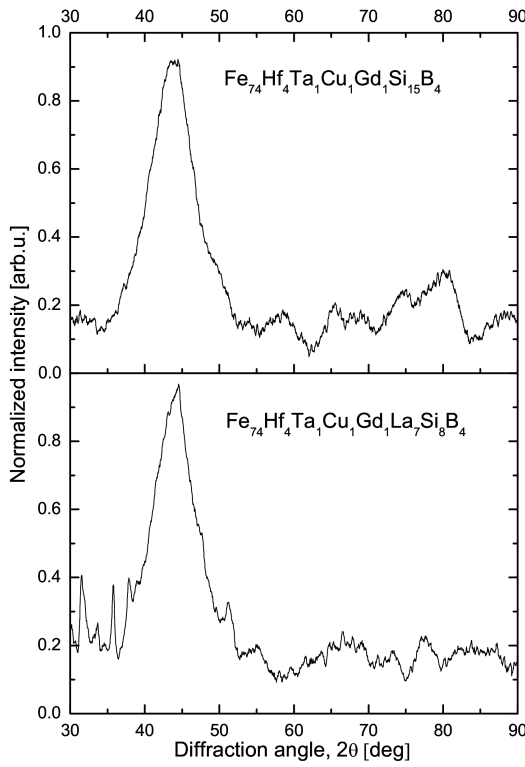


Fig. 1. X-ray diffraction patterns for as-cast $\text{Fe}_{74}\text{Hf}_4\text{Ta}_1\text{Cu}_1\text{Gd}_1\text{La}_x\text{Si}_{15-x}\text{B}_4$ alloys.

for both samples. The XRD patterns did not reveal any other diffraction peaks.

Temperatures of the first crystallization onset estimated from the DSC data collected for each alloy were 823 K and 853 K for $x = 0$ and 7, respectively. Temperatures of the first crystallization peak, corresponding to the formation of bcc-iron phase, occurred at 863 K for $x = 0$ and 878 K for $x = 7$. They could be considered as an upper threshold of the working temperature of the devices manufactured from the alloys. However, if we need to have material properties linked to the amorphous state unchanged, extra care should be taken as annealing below the crystallization onset for a sufficient period of time may also lead to crystallization.

The Mössbauer spectra were fitted with the hyperfine field distributions method, using NORMOS.dist program. The results are presented in Fig. 3 and in Table. The main parameters determined were: average hyperfine field determined from the entire distribution, $\langle H \rangle$; hyperfine field H_{main} corresponding to the major peak of the probability distribution of hyperfine field, $P(H)$; hyperfine distribution width Γ ; D23 parameter which determines the intensity ratio of the second to third line in the elementary sextet of hyperfine field distribution. Calculations were performed for $P(H)$ consisting of 40 such sextets, which hyperfine field increases by 1 T in each consecutive step of $P(H)$ distribution. Linewidth of elementary sextet was 0.31 mm/s.

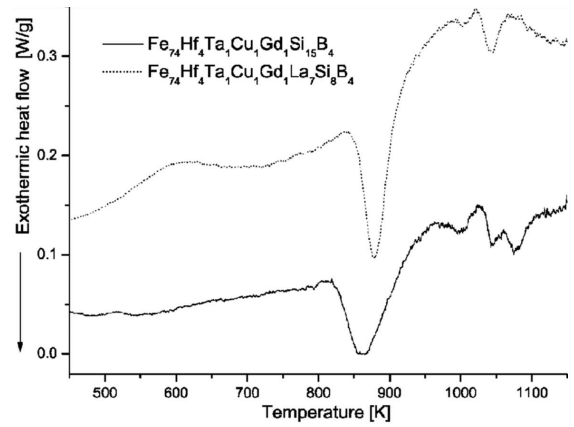


Fig. 2. Isochronal DSC curves for the as-quenched samples recorded at heating rate of 10 K/min.

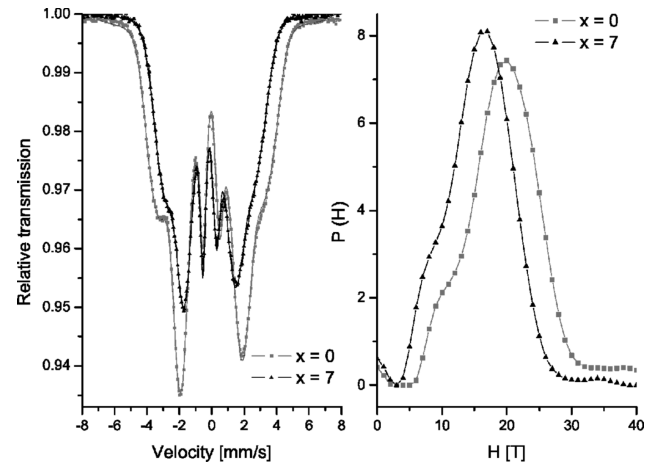


Fig. 3. Mössbauer spectra (left) and corresponding hyperfine field distributions (right) for the studied $\text{Fe}_{74}\text{Hf}_4\text{Ta}_1\text{Cu}_1\text{Gd}_1\text{La}_x\text{Si}_{15-x}\text{B}_4$ alloys.

In theory, D23 parameter may change its values from 0 to 4. When D23 equals to zero, the spins are oriented perpendicular to the sample surface, while $D23 = 4$ indicates that spins are lying in the sample plane. $D23 = 2$ corresponds to random spin orientation. The error of D23 parameter determination is usually significant and its typical values are in the range of ± 0.1 to 0.2.

TABLE

Comparison of the main parameters determined from the hyperfine field distributions for $\text{Fe}_{74}\text{Hf}_4\text{Ta}_1\text{Cu}_1\text{Gd}_1\text{La}_x\text{Si}_{15-x}\text{B}_4$ ($x = 0, 7$).

Composition	$x = 0$	$x = 7$
$\langle H \rangle$ [T]	19.9	15.7
H_{main} [T]	20.0	16.5
Γ [T]	6.5	5.3
D23 [arb.u.]	3.39	2.27

Both spectra (Fig. 3) for which the hyperfine parameters were determined, consist of a broadened sextet, which is characteristic of ferromagnetic amorphous phase. There were no additional components with narrow lines and larger hyperfine fields observed in the analyzed spectra, which implicates the absence of nanocrystalline phases in the samples studied.

As we can see in Fig. 3, hyperfine fields distributions $P(H)$, extracted from the spectra of amorphous samples with $x = 0$ and $x = 7$ are quite similar. They consist of the main peak with bell-like, symmetrical shape occurring at about 20 T for $x = 0$ and 16.5 T for $x = 7$. In both samples, near the main peak of $P(H)$, there is a slightly smaller peak at lower hyperfine field, 10 T, which is rather poorly separated from the main peak. The peak at 10 T probably corresponds to the regions depleted in Fe atoms, and thus the hyperfine field is reduced.

If we compare the data given in Table, the D23 parameter value of 3.39 for $x = 0$ suggests that spins in this sample are oriented preferentially near the ribbon plane, while in the sample with $x = 7$, the value of D23 is 2.27 which suggest that the spins are oriented nearly at random.

4. Magnetic properties

Magnetic hysteresis loops for the investigated alloys were collected with a vibrating sample magnetometer and shown in Fig. 4. It was found that the coercivity was about 12 A/m for $x = 0$ and 82 A/m for $x = 7$ at 300 K and about 600 A/m for $x = 0$ and 1200 A/m for $x = 7$ at 400 K. Remanence also changed with temperature, amounting to 0.64 T for $x = 0$ and 0.36 T for $x = 7$ at 300 K, while at 400 K it was 0.43 and 0.11 T for $x = 0$ and $x = 7$, respectively.

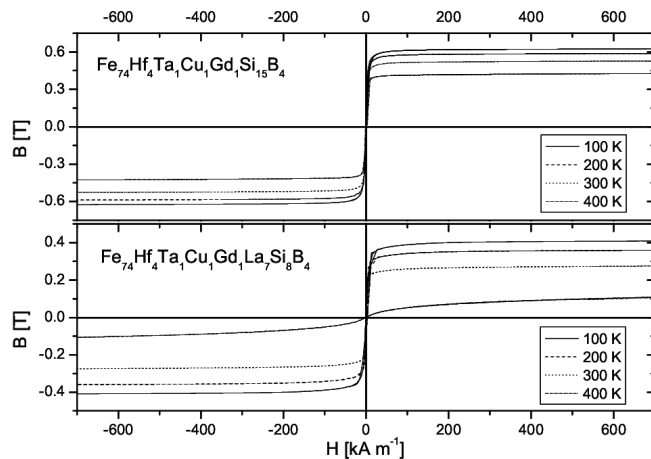


Fig. 4. Magnetic hysteresis loops for as-quenched $\text{Fe}_{74}\text{Hf}_4\text{Ta}_1\text{Cu}_1\text{Gd}_1\text{La}_x\text{Si}_{15-x}\text{B}_4$ alloys recorded with a vibrating sample magnetometer.

Temperature dependences of magnetization were shown in Fig. 5. The temperature dependence of magnetization was recorded at the non-saturating field of 5 mT

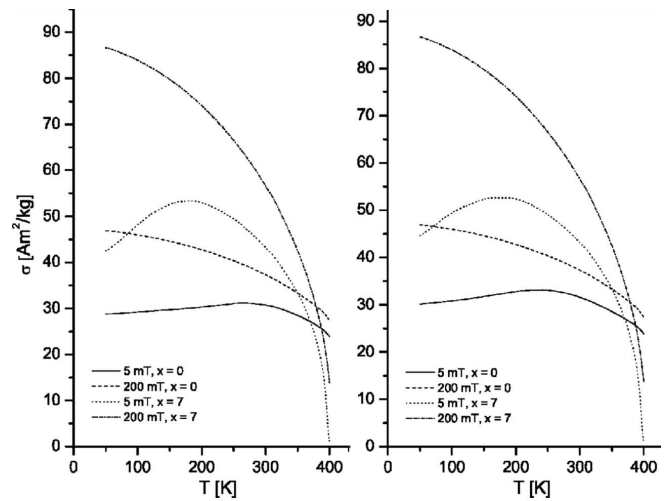


Fig. 5. Temperature dependence of field-cooled (left) and zero-field cooled (right) magnetization for $\text{Fe}_{74}\text{Hf}_4\text{Ta}_1\text{Cu}_1\text{Gd}_1\text{La}_x\text{Si}_{15-x}\text{B}_4$ alloys recorded at two magnetic fields: 5 and 200 mT.

and a field 200 mT, for which the magnetic saturation was obtained. The appropriate field values for the experiment were found from the magnetic hysteresis loops shown in Fig. 4. The study revealed that the maximum of field-cooled $M = f(T)$ dependence occurs at 256.5–272.0 K for $x = 0$ and 165.9–191.7 K for $x = 7$. If the $M = f(T)$ curves were obtained without magnetic field applied during sample cooling, the maximum occurred at 227.4–250.6 K for $x = 0$ and 148.6–202.5 K for $x = 7$. Comparison of field-cooled and zero field-cooled temperature dependences of magnetization revealed no spin freezing effects in the materials studied.

Similar amorphous alloy, $\text{Fe}_{80}\text{B}_{11}\text{Si}_9$ studied by De-Cristofaro [11] is reported to exhibit the room temperature saturation induction of 1.59 T. In contrast, the alloy investigated in the current work with $x = 0$ exhibits the saturation induction at 300 K of only 0.67 T while the Fe content is comparable in both cases. As we can see from Fig. 5, above the temperature of about 187 K, the material has typical ferromagnetic character. It resembles the magnetization versus temperature plots obtained for $\text{Fe}_{80-x}\text{B}_{20}\text{Gd}_x$, $x = 11-16$ within the two-sublattice mean-field model reported by Hassini et al. [12]. The authors propose non-collinear ferrimagnetic structure of the Gd and Fe sublattices, that could be responsible for the substantial decrease of saturation induction in the alloys studied. The Curie point, defined as a tangent to the $M = f(T)$ curve recorded under non-saturating conditions (i.e., 5 mT), of $x = 7$ alloy was found to appear at 399 K, while the sample without La has its T_c above the measurement range, 400 K. It is shown that La addition of 7 atomic percent has a beneficial effect of shifting the Curie point towards lower temperatures together with magnetization magnitude increase from 37.3 to 56.5 Am^2/kg at 300 K, field-cooled (200 mT) condition.

5. Conclusions

In the present work, a novel composition of $\text{Fe}_{74}\text{Hf}_4\text{Ta}_1\text{Cu}_1\text{Gd}_1\text{La}_x\text{Si}_{15-x}\text{B}_4$ metallic glass was investigated.

XRD diffractometry and Mössbauer spectroscopy confirmed amorphous structure of the samples, which is stable up to 823 K and 853 K for $x = 0$ and $x = 7$, respectively.

Temperature dependences of magnetization together with saturation induction estimated from recorded hysteresis loops suggests ferrimagnetic order with two magnetic sublattices, that have to be verified by further analysis.

It was found that room-temperature coercivity is nearly 7 times lower in La-deficient alloy. La addition results in a decrease of the Curie point together with the increase of magnitude of magnetization.

Acknowledgments

The task was co-financed from the European Union funds under the European Social Fund.

References

- [1] A. Wang, Q. Man, M. Zhang, H. Men, B. Shen, S. Pang, T. Zhang, *Intermetallics* **20**, 93 (2012).
- [2] M. Iqbal, J. Akhter, H. Zhang, Z. Hu, *J. Non-Cryst. Solids* **354**, 5363 (2008).
- [3] K. Kim, P. Warren, B. Cantor, *J. Non-Cryst. Solids* **317**, 17 (2003).
- [4] R. Caballero-Flores, V. Franco, A. Conde, K.E. Knippling, M.A. Willard, *Appl. Phys. Lett.* **96**, 182506 (2010).
- [5] M. Idbenali, N. Selhaoui, L. Bouirden, C. Servant, *J. Alloys Comp.* **456**, 151 (2008).
- [6] V. Raghavan, *J. Phase Equil. Diff.* **33**, 400 (2012).
- [7] V. Raghavan, *J. Phase Equil.* **22**, 158 (2001).
- [8] R.J. Highmore, A.L. Greer, *Nature* **339**, 363 (1989).
- [9] L.F. Bao, F.X. Hu, L. Chen, J. Wang, J.R. Sun, B.G. Shen, *Appl. Phys. Lett.* **101**, 162406 (2012).
- [10] S. Huang, D. Wang, Z. Han, Z. Su, S. Tang, Y. Du, *J. Alloys Comp.* **394**, 80 (2005).
- [11] N. DeCristofaro, *MRS Bull.* **23**, 50 (1998).
- [12] A. Hassini, H. Lassri, A. Bouhdada, M. Ayadi, R. Krishnan, I. Mansouri, B. Chaker, *Physica B Condens. Matter* **275**, 295 (2000).